Available online at www.sciencedirect.com
SCIENCE DIRECT®
Earth and Planetary Science Letters 243 (2006) 53–60
EPSL
www.elsevier.com/locate/epsl

An integrated approach for determining the origin of magnetite nanoparticles

Damien Faivre [a,*], Pierpaolo Zuddas [b,1]

[a] *Laboratoire de Géochimie des Eaux, CNRS UMR 7047, Université Denis Diderot and Institut de Physique du Globe de Paris, case postale 7052, 2 place Jussieu, 75251 Paris cedex 05, France*
[b] *PaléoEnvironnement & PaléobioSphère, CNRS UMR 5125, Université Claude Bernard, 43 bd du 11 Novembre 1918, 69622 Villeurbanne cedex, France*

Received 30 December 2004; received in revised form 19 December 2005; accepted 6 January 2006
Available online 13 February 2006
Editor: V. Courtillot

Abstract

The criteria to assess the origin of magnetite are of prime importance because of their significance as biomarkers for extraterrestrial life and paleoenvironmental indicators. It is still unclear if morphology and magnetic properties of crystals do quantitatively allow differentiating abiotic from biotic magnetite crystals of nanometer size. In this study, inorganic magnetite nanocrystals synthesized under controlled experimental aqueous conditions are compared with biogenic magnetite of similar size and morphology formed by magnetotactic (intracellular magnetite) and other (extracellular magnetite) bacteria. Structural properties such as oxygen isotope fractionations and crystal size distributions were explored. Not surprisingly, none of the single properties are able to differentiate inorganic crystals from those having a bacterial origin, either specifically extracellular or specifically intracellular. However, oxygen isotope fractionation allows the differentiation between abiotic and biotic magnetite when the temperature of formation is known and when it does not fall into a crossing region ($35 \leq T$ (°C) ≤ 55) while crystal size distributions discriminate inorganic from intracellular magnetite. Therefore, a combination of these two properties may be a successful tool for an accurate determination of a reliable biogenicity criterion.

Keywords: nanogeochemistry; magnetite; biogenicity criterion; oxygen isotopes; crystal size distributions

1. Introduction

The extensive debate about a possible biogenic origin of nano-sized magnetite crystals in the Martian meteorite ALH84001 emphasized that bacterial magnetite cannot always be obviously differentiated from inorganic magnetite (see among others [1–7]). Magnetotactic bacteria display one of the clearest behavioural responses to the geomagnetic field of any living organism, and are one of the few known prokaryotes which have the ability to intracellularly produce magnetic nanocrystals [8,9]. Magnetic bacteria provide an important supply of nano-sized grained magnetite to sediments, where these are supposed to be preserved after bacterial death [10–12]. Fossil bacterial magnetosomes, termed magnetofossils [13,14], have the same morphology

* Corresponding author. Present address: Department of microbiology, Max Planck Institute for marine microbiology, Celciusstrasse 1, 28359 Bremen, Germany. Tel.: +49 421 2028 748; fax: +49 421 2028 580.
E-mail addresses: dfaivre@mpi-bremen.de (D. Faivre), zuddas@ipgp.jussieu.fr (P. Zuddas).
[1] Present address: IPGP, 4 place Jussieu, 75252 Paris cedex 05, France.

0012-821X/$ - see front matter © 2006 Elsevier B.V. All rights reserved.
doi:10.1016/j.epsl.2006.01.012

and crystal structure as the crystal in the living bacteria [15].

However, magnetite found in sediments and sedimentary rocks may also have an authigenic origin as phases formed in situ by abiotic processes [16,17]. A large number of works have reported nanometric-sized bacterial (intracellular and extracellular) magnetite (see for example [18–21]). The number of studies reporting magnetite formed inorganically from aqueous solutions increases because of the rising interests for nanosciences [22,23] and biotechnologies [24,25]. Some of these studies have emphasized the role of pH and ionic strength on the precipitation of magnetite nanocrystals and specifically on the dimension of the formed crystals. In addition, experimental synthesis routes have been suggested to understand the reaction pathway or to model environmental conditions or particles properties (see exhaustive references in Cornell and Schwertmann [26]). Numerous synthesis methods allowing magnetite formation in aqueous media without any control of the parent solution have been reported [7,26,27]. However, specific crystals properties cannot, in this case, be related to the formation conditions as the chemical affinity changes during the crystal growth. Particles obtained by those synthetic pathways have for example various morphologies and dimensions that lead to broad crystal size distributions (CSDs) [7]. Such synthesis routes therefore lead to crystals that can be similar to crystals formed by Bio-Induced Mineralization (BIM). Solution control, via pH-control [28–30], via the addition of proteins produced by magnetotactic bacteria [31] or via the use of micro-environments such as phosphatidycholine unilamellar vesicles [32], can affect the formed particles. Indeed, crystals may have size, morphology, structure, chemical composition, and/or CSD that are related to their conditions of formation as it is the case in Bio-Controlled Mineralization (BCM).

In this study, the oxygen isotopic fractionation between water and nanometer-sized abiotic magnetites formed in the laboratory at low temperature and under controlled chemical affinity were measured in order to better understand the acquisition of specific oxygen isotope compositions by natural magnetite. With the help of previous experimental studies, we have also tried to connect geochemical properties to the formation conditions of the nanocrystals.

2. Experimental approach

Rate and mechanism of heterogeneous reactions are a function of the reaction chemical affinity. Classically mineral dissolution and precipitation reaction rates have most often been expressed in terms of a functional dependence. Using the Lasaga formalism [33] the rate of reaction R_{net} and the chemical affinity A can be linked by:

$$R_{net} = R_{+}(1-e^{-A/RT}) \quad (1)$$

where R is the perfect gas constant, R_{+} is the rate for the forward reaction in Eq. (2) and T is the temperature (in K). A variation of the chemical affinity might have an important effect on the global rate of the reaction affecting the reaction pathway and the mechanism of mineral formation. These changes in reaction mechanism and rates will in turn affect the geochemical properties of the product of reaction, being in our case the formed mineral.

A series of controlled experimental magnetite precipitations were carried out by co-precipitation of ferrous and ferric ions in aqueous solution under a constant pH condition [28]. The selected methodology allowed forming magnetite nanocrystals under constant and controlled affinity conditions. At a given constant pH, the overall reaction of magnetite precipitation can be schematically represented by a simplified mass balance equation:

$$2Fe^{3+} + Fe^{2+} + 4H_2O \underset{R_-}{\overset{R_+}{\rightleftharpoons}} Fe_3O_4 + 8H^+ \quad (2)$$

where R_{+} is the rate of the forward reaction and R_{-} is the rate of the reverse reaction. Since the reaction produced protons, pH was held constant by an automatic adding of sodium hydroxide solution. These experimental conditions were suitable to form magnetite at low temperature under constant chemical affinity. Classically, the state of saturation, Ω, is defined by:

$$\Omega = \frac{a_{Fe^{2+}} a^2_{Fe^{3+}}}{a^8_{H^+} K_S} \quad (3)$$

where a_X is the activity of the species X and K_S is the thermodynamic magnetite solubility. Typical values for K_S are in the range between $10^{9.61}$ and $10^{12.02}$ [27,34]. It was however difficult to estimate the real saturation state in our experimental conditions as solubility constants of magnetite are known at high temperature [34,35] and extrapolations to low temperature are hazardous. In addition, recent solubility estimations on nanometer size minerals [22,23,36] showed that at this scale, mineral solubility is several orders of magnitude different from that evaluated at the micro- and millimetre scale. An operative empirical and experimental way to verify the magnetite-solution equilibrium condition was therefore to use the total iron concentration [28].

The effect of temperature was here specifically investigated to evaluate its effect on the oxygen isotopic composition and on crystal dimension. Analyses of oxygen isotopic compositions were performed by fluorination methods [37]. Solutions containing magnetite nanocrystals were carefully washed and evaporated under vacuum directly after the wash. These are crucial steps for obtaining reliable $\delta^{18}O$ for fine-grained, low-temperature precipitates [38,39]. In our case, the oxygen isotopic value could be modified by salts used to maintain ionic strength. As checked by TEM, nitrate salts were always completely removed from samples to be analyzed for isotope fractionation measurements. When present in unwashed samples, nitrates form a well recognizable gangue around magnetite nanocrystals. Nearly 20 mg of solid material were necessary for each analysis. The solids were placed in Ni tubes, evacuated and preheated at 150 °C for 4 h to remove adsorbed water. Tubes were then heated to 650 °C for 12 h with a 5 times excess of BrF_5. Oxygen was then separated from other gases by passage through liquid nitrogen traps that retained other volatile gases by condensation. Oxygen was trapped on a zeolite-filled cold finger cooled with liquid nitrogen, quantified by measuring the volume of the extracted oxygen in order to calculate the yield of the isotopic analyses and finally transferred to the mass spectrometer (VG Optima) where intensities associated to the ions of masses 32 and 34 were measured. Yields are calculated as the ratio of experimental and theoretical yield. Based on the perfect gas law, a theoretical yield 8.63 μmol of O_2/mg of magnetite is obtained. Runs with yields greater than 90% were accepted, while the others were rejected. Repetitive analyzes of NBS 28 (quartz, $\delta^{18}O=9.35\pm0.11$‰, $n=10$) and Circe 93 (basaltic glass from mid-oceanic ridge, $\delta^{18}O=5.72\pm0.13$‰, $n=25$) were used as calibration procedure (true values: NBS 28, $\delta^{18}O=9.58$ and Circe 93, $\delta^{18}O=5.72$) with an overall error of ±0.2‰. The $\delta^{18}O$ of water, prior to and after magnetite precipitation, were determined by CO_2–H_2O equilibration. One or two drops of 100% H_3PO_4 were previously added to the solutions to neutralize the alkaline media used for precipitation.

3. Crystal properties and formation conditions

3.1. Conditions for abiotic magnetite formation

In natural Earth surface environments, total iron concentrations change from 0.1 $\mu mol\times L^{-1}$ in superficial oxidative conditions to 100 $mmol\times L^{-1}$ in oxygen-free pore seawaters [40,41]. Using the numerical thermodynamic model EQ3NR [42], we found that magnetite is the only mineral stable phase at pH of 10.5 for a large range of total iron concentration (i.e. from 1 $mmol\times L^{-1}$ to 1 $mol\times L^{-1}$) when the Fe^{2+}/Fe^{3+} ratio is 0.5 and for a large range of temperature (5 to 70 °C) (Table 1). This stands clearly in contrast with previous experimental observations [28] where it was found that at 25 °C, when parent solutions with iron stoichiometric Fe^{2+}/Fe^{3+} ratio of 0.5 have a total iron concentration lower than about 20 $mmol\times L^{-1}$, goethite particles (α-FeOOH) coexist with poorly crystallized matrix of iron oxides and hydroxides, and with some magnetite crystals. Nanometer-sized magnetite was the only mineral formed when the total iron concentration exceeds 30 $mmol\times L^{-1}$ in the

Table 1
Summary of measurements at the total iron concentration of 0.150 M (Fe(II)/Fe(III)=0.5)

Sample	T (°C)	$\delta^{18}O_m$ (‰)	$\delta^{18}O_{w_1}$ (‰)	$\delta^{18}O_{w_2}$ (‰)	$10^3\ln\alpha_{m-w}$ (1σ)
IST5/1	5.5	−7.50	−6.01	−5.99	−1.13 (0.53)
		−7.49			
IST5/2	5.6	−6.56	−5.88	−5.80	
		−6.63			
IST15/1	15.1	−6.76	−5.96	−5.92	−0.88 (0.53)
		−6.87			
		−7.19			
IST15/2	15.2	−6.12	−5.80	−5.76	
		−5.97			
		−6.18			
IST25/1	24.5	−7.47	−6.62	−6.60	−0.83 (0.27)
		−7.09			
IST25/2	24.5	−7.60	−6.53	−6.51	
IST30/1	29.8	−5.92	−6.01	−5.91	0.08 (0.33)
		−6.42			
IST30/2	29.8	−5.77	−6.16	−6.14	
		−5.78			
IST40/1	39.6	−6.14	−6.22	−6.15	−0.08 (0.37)
		−5.91			
		−5.81			
IST40/2	39.6	−6.69	−6.04	−5.99	
		−6.35			
IST50/1	49.3	−6.21	−6.08	−6.04	0.03 (0.19)
		−6.01			
IST50/2	49.3	−5.83	−6.06	−6.00	
IST60/1	58.7	−5.16	−6.25	−5.99	0.89 (0.56)
		−4.81			
IST60/2	58.7	−5.88	−6.24	−6.18	
IST70/1	69.0	−2.08	−4.29	−4.05	1.41 (0.62)
IST70/2	69.0	−3.23	−4.27	−4.04	
		−2.98			

Results of isotope analyses are given as fractionation of magnetite ($\delta^{18}O_m$), water ($\delta^{18}O_w$) and as fractionation factors ($10^3\ln\alpha_{m-w}$), measured between magnetite nanocrystals and water. Analyses are performed for water in triplicates, prior to reaction start ($\delta^{18}O_{w_1}$) and at the end of the reaction ($\delta^{18}O_{w_2}$). The mean value is used. Each measurement has been at least duplicated. Mean values of fractionation factors ($10^3\ln\alpha_{m-w}$) are given in column with variance in brackets.

absence of inorganic and organic catalysts. This indicates that present available thermodynamic data do not accurately scale down to low temperature conditions to operatively establish a proper thermodynamic equilibrium condition in the case of magnetite crystals having nanometer size.

Inorganic syntheses were carried out under $[Fe]_{tot}$ = 150 mmol × L^{-1}. This concentration was shown to exclusively produce magnetites [28,43] that have an average dimension of about 10 nm. This dimension is in the same order of magnitude than biogenic magnetites studied in previous oxygen isotope studies [44,45]. This size was not changed when the temperature of synthesis is varied from 5 to 69 °C (Fig. 1) indicating a similar reaction mechanism under pure abiotic conditions. Furthermore, electron diffraction patterns, Fourier analysis of high resolution images and EDX have confirmed that only magnetite was formed over the whole temperature reported in this study.

Structural properties have commonly been proposed to determine magnetite nanocrystals origin [5,46–51]. Indeed, biogenic magnetite crystals have high chemical purity, narrow size ranges, species-specific crystal morphologies and exhibit specific arrangements within the cell. These features indicate that the formation of biogenic magnetite by magnetotactic bacteria requires precise biological control and should leave an indelible imprint to the particle. Nanocrystals formed in our inorganic conditions at constant chemical affinity are essentially free of internal defects as shown in Fig. 1 and in Faivre et al. [43]. The absence of internal defects has also been observed in BCM of magnetite [5,7]. Typical morphologies obtained in our study are cubo-octahedral. This form is a combination of the isometric forms {1 1 1} and {1 0 0} as showed in Fig. 1. Since a simple low-temperature, organic-free solution, reflecting sedimentary conditions, can lead to the precipitation of well defined crystals, such as those observed for BCM [8,21,52–55] we propose that there is no need for biological intervention to control the shape of the nanocrystals of magnetite. Our inorganic crystals have different morphology than the critical crystals produced by the magnetotactic bacteria of strain MV-1. However, Golden et al. [51] have shown that ALH84001 crystals were elongated cubo-octahedron, not truncated hexa-octahedron (the MV-1 crystals morphology). They have shown that thermal decomposition products of Fe-rich carbonate, a high temperature process, produced by inorganic hydrothermal precipitation in laboratory experiments can form particles with morphology similar to that of particles observed in ALH84001. However, the temperature in the meteorite is also controversial (see for example [56,57]). Here, we show that even low temperature inorganic aqueous syntheses can produce crystals with a similar morphology to that found in the meteorite ALH84001. To our knowledge, no previous low temperature inorganic processes producing crystals having similar morphologies than the ones from the ALH84001 were reported. The crystal morphology seems thus not to be a univocal parameter to be used as biogenicity criterion, at least in the case of the ALH84001 meteorite.

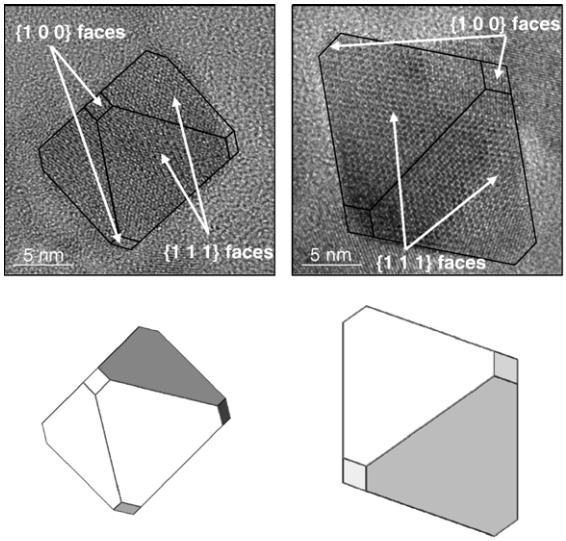

Fig. 1. Typical high resolution transmission electron micrographs of magnetite crystals. Overprinted are the crystallographic indexes and the faces of simulated crystals. Simulations are based on electronic diffraction properties and on the hypothesis of cubo-octahedron [43]. Zone axes are respectively [1 1 2], and [0 1 1]. The simulated crystals showed good agreement with the typical magnetite crystals shown.

3.2. Crystal origin determination

Fig. 2 shows that the magnetite–water oxygen isotopic fractionation (α_{m-w}) obtained in our abiotic conditions increases by about 2.5‰ as function of the temperature in the low temperature range, between 5 and 69 °C. Fig. 3 reports the parameterization of these experimental results and associate them to that of Mandernack et al. and Zhang et al. [44,45] on biogenic magnetite where its is found that the biogenic magnetite–water oxygen isotope fractionation decreases by about 3.5‰ between 4 and 70 °C. Biogenic fractionation factors are obtained from both bacterial magnetite produced intracellularly (BCM magnetite) [44] and extracellularly (BIM magnetite) [45]. Fig. 3 clearly shows that abiotic magnetite give fractionation factors

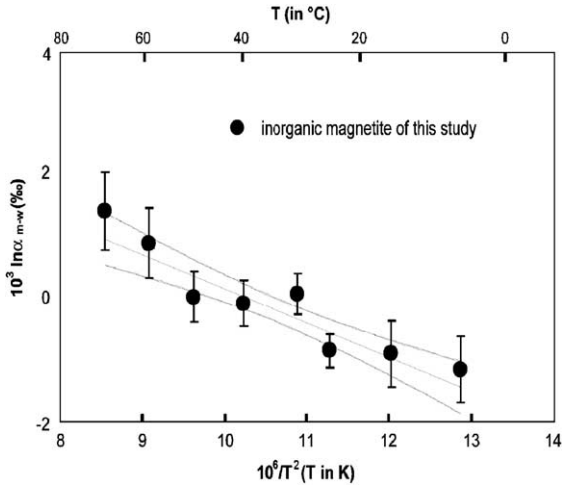

Fig. 2. Oxygen isotope fractionation factor between magnetite and water (10^3 $\ln\alpha_{m-w}$) plotted as a function of temperature ($10^6/T^2$, T in K). The generic equation of the hyperboles is: $y=cx^2+ax+b$ (upper limit: $a=-1.59$, $b=11.43$, $c=0.048$, lower limit: $a=0.50$, $b=-0.15$, $c=-0.048$).

that increase as a function of temperature whereas biological magnetite fractionation factors decrease as a function of temperature suggesting that oxygen isotope composition of magnetite is a suitable tool for magnetite genesis biosignature if the formation temperature is known. However, such a tool cannot easily be applied if the temperature of formation of the crystal falls in the crossing region corresponding to the temperature range between 35 and 55 °C. The large difference between abiotic and biotic curves at temperatures from 5 to about 25 °C enhances the interest of such a diagnostic tool at these temperatures. Therefore, differentiation between biotic and abiotic magnetite is based on both biologically controlled magnetite produced intracellularly by magnetotactic bacteria [44] and biologically induced magnetite produced extracellularly by thermophilic bacteria [45]. Another criterion would thus be necessary to specifically differentiate abiotic magnetite from intracellularly formed magnetite and abiotic magnetite from extracellularly formed magnetite.

CSD of minerals may discriminate the condition of mineral formation as crystal growth history has an impact on the particle dimension [58]. Specific properties of the whole population are naturally more reliable than properties of a given sample of this population (morphology) since they are based on a greater number of crystals [59]. Fig. 4 shows schematic CSDs for both inorganic and biogenic populations of magnetite nanocrystals. Inorganic particles exhibited a log-normal CSD. Log-normal CSDs are asymmetric and with cut-off toward smaller sizes. When the solution chemistry is variable, magnetite crystals are formed under conditions of variable affinity, and a broadening of the CSD is observed. CSDs for biogenic magnetite populations of three different strain of magnetotactic bacteria also exhibited asymmetric CSDs, but inverse log-normal CSDs i.e. with sharp cut-offs toward larger size [7]. The difference between the mode and the mean

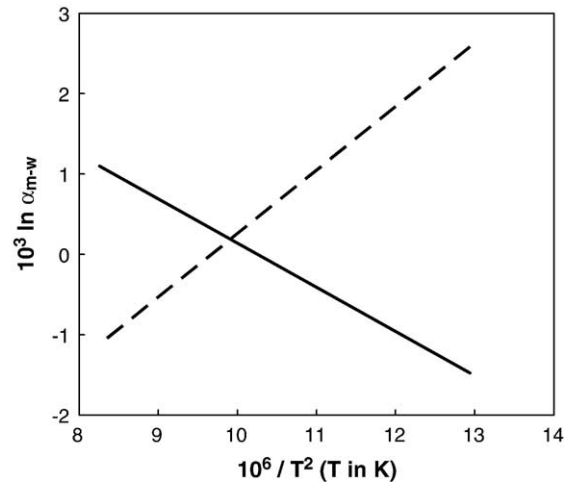

Fig. 3. Schematic magnetite–water oxygen isotope fractionation (α_{m-w}) diagram; inorganic fractionation of this study (bold line) increases by about 2.5‰ between 5 and 69 °C according to (T in K): 10^3 $\ln\alpha_{m-w}=-0.55$ (±0.13) ($10^6/T^2$)+5.64 (±1.42), whereas biogenic magnetite–water oxygen isotope fractionation (dashed line) [44,45] decreases by about 3.5‰ between 4 and 70 °C according to (T in K): 10^3 $\ln\alpha_{m-w}=0.79$ ($10^6/T^2$)−7.64.

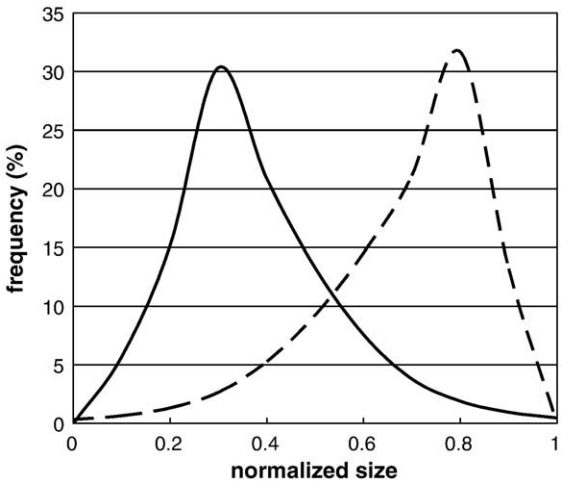

Fig. 4. Schematic crystal size distributions for populations of magnetite nanocrystals. Biogenic populations (dashed line) show inverse log-normal CSDs [7], whereas inorganic populations (bold line) show log-normal CSDs [7,43] and are usually a little broader. The size of crystals is normalized to the larger crystal of the respective populations.

of the normalized population (size normalized by the maximal crystal size of the population) is also usually greater for the biogenic population. This feature, however, might not be statistically meaningful. The opposite asymmetry of the CSDs from biogenic and nonbiogenic synthesis is therefore the remaining parameter. Therefore, the statistical analysis of size might provide a robust criteria for distinguishing between intracellular biogenic and other crystals (extracellular and nonbiogenic particles) [7,60].

4. Implications and conclusions

At standard Earth surface temperatures, the formation of magnetite nanocrystals is kinetically a function of the ferrous iron [28,61]. In sedimentary environmental conditions, inorganic nanocrystals of magnetite would be possible in specific systems where the iron concentration is particularly high. Recent direct pore water measurements have indicated that especially in the case of environmental accident [41], high level of iron are measured. The reaction pathway including ferrous iron activity control on magnetite formation is similar to that observed for biogenic magnetite formation. Indeed, Frankel et al. [62] found that ferric oxides are first formed intracellularly and the only in a second step a mineral transformation produces nanocrystal of magnetite. Therefore, it is possible that a single and universal mechanism could be responsible for magnetite formation in aqueous environmental conditions, but probably with different ferric intermediates.

Criteria of biogenicity have to be defined in the case of similar sizes when magnetic properties might not be sufficient to differentiate inorganic and biogenic particles. Structural properties have consequently been studied. Cubo-octahedral morphologies are observed for crystals formed by inorganic synthesis, also for crystals found in the Martian meteorite ALH 84001. Therefore, in that case, morphology cannot be used as biogenicity criterion. Fractionation factors of oxygen isotopes during magnetite precipitation at different temperature allow the differentiation between biotic and abiotic magnetite without the limit of the crossing region. Moreover, opposite asymmetries of the CSDs from biogenic and nonbiogenic synthesis are observed. Finally, the analysis of CSDs should thus provide a criterion to distinguish BCM crystals from others (BIM and inorganic particles). We therefore propose a combination of oxygen isotopic property and crystal size distribution as a tool for an accurate determination of a reliable biogenicity criterion. Isotopic fractionation and CSDs have yet to be evaluated for other mechanisms of magnetite formation to confirm or not the possibility of using such a biogenicity criterion.

Acknowledgments

The studies would not have been possible without the help of numerous collaborators. We would specifically like to thank N. Menguy for his help with electron microscopy, P. Agrinier for his help with oxygen isotope analysis and C. Gros for her help with English. The help of O. Lopez, F. Guyot, and R. Hellmann were particularly appreciated, both for scientific and “formal” remarks. Reviews by Prof. J. Bradley, Prof. J. L. Kirschvink and two anonymous reviewers were appreciated. We also thank the editor, V. Courtillot, for handling on our manuscript. This, indeed, was not an easy task. This research was financially supported by a French MENRT Fellowship and by IPGP BQR 2000 and University of Paris 7 BQR 2001 grants. This is the IPGP contribution no 2107.

References

[1] J.P. Bradley, R.P. Harvey, J.Y. McSween, D.S. McKay, J.E. Gibson, K. Thomas-Keprta, H. Vali, No ‘nanofossils’ in Martian meteorite, Nature 390 (6659) (1997) 454–456.
[2] L. Becker, B. Popp, T. Rust, J.L. Bada, The origin of organic matter in the Martian meteorite ALH84001, Earth Planet. Sci. Lett. 167 (1999) 71–79.
[3] J.L. Kirschvink, A.T. Maine, H. Vali, Paleomagnetic evidence of a low-temperature origin of carbonates in the Martian meteorite ALH 84001, Science 275 (1997) 1629–1633.
[4] D.S. McKay, E.K. Gibson Jr., K.L. Thomas-Keprta, H. Vali, C.S. Romanek, S.J. Clemett, X.D.F. Chilier, C.R. Maechling, R.N. Zare, Search for past life on Mars: possible relic biogenic in Martian meteorite ALH84001, Science 273 (1996) 924–930.
[5] K.L. Thomas-Keprta, D.A. Bazlinski, J.L. Kirschvink, S.J. Clemett, D.S. McKay, S.J. Wentworth, H. Vali, E.K. Gibson Jr., C.S. Romanek, Elongated prismatic crystals in ALH84001 carbonate globules: potential Martian magnetofossils, Geochim. Cosmochim. Acta 64 (23) (2000) 4049–4081.
[6] A.H. Treiman, C.S. Romanek, Bulk and stable isotopic compositions of carbonate minerals in Martian meteorite Allan Hills 84001: no proof of high formation temperature, Meteorit. Planet. Sci. 33 (1998) 737–742.
[7] B. Devouard, M. Posfai, X. Hua, D.A. Bazylinski, R.B. Frankel, P.B. Buseck, Magnetite from magnetotactic bacteria: size distributions and twinning, Am. Min. 83 (1998) 1387–1398.
[8] E. Baeuerlein, Biomineralization of unicellular organisms: an unusual membrane biochemistry for the production of inorganic nano- and microstructures, Angew. Chem. Int. Ed. 42 (6) (2003) 614–641.
[9] D. Schüler, The biomineralisation of magnetosomes in *Magnetospirillum gryphiswaldense*, Int. Microbiol. 5 (2002) 209–214.
[10] P.P. Hesse, Evidence for bacterial palaeoecological origin of mineral magnetic cycles in oxic and sub-oxic Tasman Sea sediments, Mar. Geol. 117 (1–4) (1994) 1–17.

[11] J.A. Peck, J.W. King, Magnetofossils in the sediment of Lake Baikal, Siberia, Earth Planet. Sci. Lett. 140 (1996) 159–172.
[12] O. Paasche, R. Lovlie, S.O. Dahl, J. Bakke, A. Nesje, Bacterial magnetite in lake sediments: late glacial to Holocene climate and sedimentary changes in northern Norway, Earth Planet. Sci. Lett. 223 (3–4) (2004) 319–333.
[13] J.L. Kirschvink, S.-B.R. Chang, Ultrafine-grained magnetite in deep-sea sediments: possible bacterial magnetofossils, Geology 12 (1984) 559–562.
[14] S.-B.R. Chang, J.L. Kirschvink, Magnetofossils, the magnetization of sediments, and the evolution of magnetite biomineralization, Annu. Rev. Earth Planet. Sci. 17 (1989) 169–195.
[15] H. Vali, J.L. Kirschvink, Magnetofossil dissolution in a paleomagnetically unstable deep-sea sediment, Nature 339 (1989) 203–206.
[16] B.A. Maher, R. Thompson, Paleomagnetic significance of the mineral record of the Chinese loess and paleosols, Quat. Res. 37 (1992) 155–170.
[17] M. Jackson, C. McCabe, M.M. Ballard, R. Vandervoo, Magnetite authigenesis and diagenetic paleotemperatures across the northern Appalachian Basin, Geology 16 (7) (1988) 592–595.
[18] D.A. Bazylinski, Synthesis of the bacterial magnetosome: the making of a magnetic personality, Int. Microbiol. 2 (1999) 71–80.
[19] J.K. Fredrickson, J.M. Zachara, D.W. Kennedy, H. Dong, T.C. Onstott, N.W. Hinman, S.-M. Li, Biogenic iron mineralization accompanying the dissimilatory reduction of hydrous ferric oxide by a groundwater bacterium, Geochim. Cosmochim. Acta 62 (19–20) (1998) 3239–3257.
[20] S. Glasauer, P.G. Weidler, S. Langley, T.J. Beveridge, Controls on Fe reduction and mineral formation by a subsurface bacterium, Geochim. Cosmochim. Acta 67 (7) (2003) 1277–1288.
[21] Y. Roh, C.L. Zhang, H. Vali, R.J. Lauf, J. Zhou, T.J. Phelps, Biogeochemical and environmental factors in Fe biomineralization: magnetite and siderite formation, Clays Clay Miner. 51 (1) (2003) 83–95.
[22] Y. Wang, C. Bryan, H. Xu, H. Gao, Nanogeochemistry: geochemical reactions and mass transfers in nanopores, Geology 31 (5) (2003) 387–390.
[23] M.F. Hochella Jr., Nanoscience and technology: the next revolution in the Earth sciences, Earth Planet. Sci. Lett. 203 (2002) 593–605.
[24] I. Safarik, M. Safarikova, Magnetic nanoparticles and biosciences, Monatsh. Chem. 133 (6) (2002) 737–759.
[25] P. Tartaj, M.D. Morales, S. Veintemillas-Verdaguer, T. Gonzalez-Carreno, C.J. Serna, The preparation of magnetic nanoparticles for applications in biomedicine, J. Phys. D: Appl. Phys. 36 (13) (2003) R182–R197.
[26] R.M. Cornell, U. Schwertmann, The Iron Oxides (Structure, Properties, Reactions, Occurrences and Uses), Wiley-VCH, Weinheim, 2003, 664 pp.
[27] R.M. Cornell, U. Schwertmann, The Iron Oxides: Structure, Properties, Reactions, Occurrences and Uses, VCH, Weinheim, 1996, 573 pp.
[28] D. Faivre, P. Agrinier, N. Menguy, P. Zuddas, K. Pachana, A. Gloter, J.-Y. Laval, F. Guyot, Mineralogical and isotopic properties of inorganic nanocrystalline magnetites, Geochim. Cosmochim. Acta 68 (21) (2004) 4395–4403.
[29] L. Vayssières, Précipitation en milieu aqueux de nanoparticules d'oxydes. Modélisation de l'interface et contrôle de la croissance, University P. et M. Curie, Paris 6, Paris, 1995.
[30] L. Vayssières, C. Chanéac, E. Tronc, J.P. Jolivet, Size tailoring or magnetite particles formed by aqueous precipitation: an example of thermodynamic stability of nanometric oxide particles, J. Colloid Interface Sci. 205 (1998) 205–212.
[31] A. Arakaki, J. Webbs, T. Matsunaga, A novel protein tightly bound to bacterial magnetite particles in *Magnetospirillum magnetotacticum* strain AMB-1, J. Biol. Chem. 278 (10) (2003) 8745–8750.
[32] S. Mann, J.P. Hannington, Formation of iron oxides in unilamellar vesicles, J. Colloid Interface Sci. 122 (2) (1987) 326–335.
[33] A.C. Lasaga, Kinetic Theory in the Earth Sciences, Princeton University Press, Princeton, 1998, 811 pp.
[34] F.H. Sweeton, C.F. Baes Jr., The solubility of magnetite and hydrolysis of ferrous ion in aqueous solutions at elevated temperatures, J. Chem. Thermodyn. 2 (1970) 479–500.
[35] S.E. Ziemniak, M.E. Jones, K.E.S. Combs, Magnetite solubility and phase stability in alkaline media at elevated temperatures, J. Solution Chem. 24 (9) (1995) 837–877.
[36] M.F. Hochella Jr., There's plenty of room at the bottom: nanoscience in geochemistry, Geochim. Cosmochim. Acta 66 (5) (2002) 735–743.
[37] R.N. Clayton, T.K. Mayeda, The use of bromine pentafluoride in the extraction of oxygen from oxides and silicates for isotopic analysis, Geochim. Cosmochim. Acta 27 (1963) 43–52.
[38] C.J. Yapp, Oxygen and hydrogen isotope variations among goethites (α-FeOOH) and the determination of paleotemperatures, Geochim. Cosmochim. Acta 51 (2) (1987) 355–364.
[39] H. Bao, P.L. Koch, Oxygen isotope fractionation in ferric oxide–water system: low temperature synthesis, Geochim. Cosmochim. Acta 63 (5) (1999) 599–613.
[40] G. Michard, Equilibres chimiques dans les eaux naturelles, Editions Publisud, Paris, 1989, 357 pp.
[41] B. Deflandre, A. Mucci, J.-P. Gagné, C. Guignard, B. Sundby, Early diagenetic processes in coastal marine sediments disturbed by a catastrophic sedimentation event, Geochim. Cosmochim. Acta 66 (14) (2002) 2547–2558.
[42] T.J. Wolery, Calculations of Chemical Equilibrium between Solutions and Minerals: the EQ3/6 Software Package: UCRL-52658, Lawrence Livermore National Laboratory, Livermore, California, 1979.
[43] D. Faivre, N. Menguy, F. Guyot, O. Lopez, P. Zuddas, Morphology of nanomagnetite crystals: implications for formation conditions, Am. Min. 90 (2005) 1793–1800.
[44] K.W. Mandernack, D.A. Bazylinski, W.C. Shanks, T.D. Bullen, Oxygen and iron isotope studies of magnetite produced by magnetotactic bacteria, Science 285 (5435) (1999) 1892–1896.
[45] C. Zhang, S. Liu, T.J. Phelps, D.R. Cole, J. Horita, S.M. Fortier, M. Elless, J.W. Valley, Physiochemical, mineralogical, and isotopic characterization of magnetite-rich iron oxides formed by thermophilic iron-reducing bacteria, Geochim. Cosmochim. Acta 61 (21) (1997) 4621–4632.
[46] D.J. Barber, E.R.D. Scott, Transmission electron microscopy of minerals in the Martian meteorite Allan Hills 84001, Meteorit. Planet. Sci. 38 (6) (2003) 831–848.
[47] J.P. Bradley, H.Y. McSween Jr., R.P. Harvey, Epitaxial growth of nanophase magnetite in Martian meteorite ALH84001: implications for biogenic mineralization, Meteorit. Planet. Sci. 33 (1998) 765–773.
[48] P.R. Buseck, R.E. Dunin-Borkowski, B. Devouard, R.B. Frankel, M.R. McCartney, P.A. Midgley, M. Posfai, M. Weyland, Magnetite morphology and life on Mars, Proc. Nat. Acad. Sci. U. S. A. 98 (24) (2001) 13490–13495.
[49] S.J. Clemett, K.L. Thomas-Keprta, J. Shimmin, M. Morphew, J.R. McIntosh, D.A. Bazylinski, J.L. Kirschvink, S.J.

Wentworth, D.S. McKay, H. Vali, E.K. Gibson Jr., C.S. Romanek, Crystal morphology of MV-1 magnetite, Am. Min. 87 (2002) 1727–1730.

[50] P. Gillet, J.A. Barrat, T. Heulin, W. Achouak, M. Lesourd, F. Guyot, K. Benzerara, Bacteria in the Tatahouine meteorite: nanometric-scale life in rocks, Earth Planet. Sci. Lett. 175 (2000) 161–167.

[51] D.C. Golden, D.W. Ming, R.V. Morris, A.J. Brearley, H.V. Lauer Jr., A.H. Treiman, M.E. Zolensky, C.S. Schwandt, G.E. Lofgren, G.A. McKay, Evidence for exclusively inorganic formation of magnetite in Martian meteorite ALH84001, Am. Min. 89 (2004) 681–695.

[52] E. Baeuerlein, Biomineralization, Wiley-VCH, Weinheim, 2000, 294 pp.

[53] D.A. Bazylinski, R.B. Frankel, Biologically controlled mineralization in prokaryotes, in: P.M. Dove, J.J. De Yoreao, S. Weiner (Eds.), Biomineralization, Reviews in Mineralogy and Geochemistry, vol. 54, Mineralogical Society of America, Geochemical Society, Washington, 2003, pp. 217–248.

[54] J.L. Kirschvink, J.W. Hagadorn, A grand unified theory of biomineralization, in: E. Bäuerlein (Ed.), The Biomineralization of Nano- and Micro-Structures, Wiley-VCH Verlag GmbH, Weinheim, 2000, pp. 139–150.

[55] D. Schüler, R.B. Frankel, Bacterial magnetosomes: microbiology, biomineralization and biotechnological applications, Appl. Microbiol. Biotechnol. 52 (1999) 464–473.

[56] J.W. Valley, J.M. Eiler, C.M. Graham, E.K. Gibson Jr., C.S. Romanek, E.M. Stolper, Low-temperature carbonate concretions in the Martian meteorite ALH84001: evidence from stable isotopes and mineralogy, Science 275 (1997) 1633–1638.

[57] J.P. Bradley, R.P. Harvey, H.Y. McSween Jr., Magnetite whiskers and platelets in the ALH84001 Martian meteorite: evidence of vapor phase growth, Geochim. Cosmochim. Acta 60 (24) (1996) 5149–5155.

[58] D.D. Eberl, V.A. Drits, J. Srodon, Deducing growth mechanisms for minerals from the shapes of crystal size distributions, Am. J. Sci. 298 (1998) 499–533.

[59] P. Vermeesch, How many grains are needed for a provenance study? Earth Planet. Sci. Lett. 224 (2004) 441–445.

[60] B. Arató, M. Pósfai, Crystal size distributions of magnetite from magnetotactic bacteria: criteria for identifying biogenic particles in rocks, Geophysical Research Abstracts, vol. 5, 2003, p.10190.

[61] J.P. Jolivet, P. Belleville, E. Tronc, J. Livage, Influence of Fe(II) on the formation of the spinel iron oxide in alkaline medium, Clays Clay Miner. 40 (5) (1992) 531–539.

[62] R.B. Frankel, G.C. Papaefthymiou, R.P. Blakemore, W. O'Brian, Fe_3O_4 precipitation in magnetotactic bacteria, Biochim. Biophys. Acta 763 (1983) 147–159.